https://doi.org/10.5194/amt-2023-265
Preprint. Discussion started: 1 February 2024

Atmospheric Measurement Techniques Discussions

Quantifying H_2S with a Picarro CRDS G2201-i and the effect of H_2S on carbon isotopes

Jessica Salas-Navarro[1], John Stix[1], J. Maarten de Moor [2,3]

[1] Department of Earth and Planetary Sciences, McGill University, 3450 University Street, Montreal, QC, H3A 0E8, Canada
[2]Observatorio Vulcanológico y Sismológico de Costa Rica, Campus Omar Dengo, Apartado Postal 2386-3000 Heredia, Costa Rica
[3]Department of Earth and Planetary Sciences, University of New Mexico, Albuquerque, Northrop Hall 141, MSC03 2040, 221 Yale Blvd. NE, NM, USA

Correspondence to: Jessica Salas-Navarro (salas15.navarro@gmail.com)

Abstract. Cavity Ring-Down Spectroscopy (CRDS) is a popular analytical method with important applications in earth sciences including volcanology. A main disadvantage of using CRDS in volcanology is that the presence of H_2S distorts some spectral lines causing errors in the measurements. In this study, we investigated the effects of H_2S on measurements using a Picarro G2201-i instrument. We defined the interferences caused by H_2S on CO_2, CH_4, and their carbon isotopic compositions. We found that 30 ppb H_2S in 1000 ppm CO_2 causes a difference of ~1.0 ± 0.2 ‰ on the $\delta^{13}C$-CO_2 measurement, while 1 ppm H_2S in 1 ppm CH_4 per causes a difference of <0.2 ‰ on the $\delta^{13}C$-CH_4 measurement; this agrees with the results from previous studies using other models of Picarro instruments. Characterizing how H_2S produces these interferences as a function of concentration, we further developed a series of equations to quantify H_2S in gas mixtures in a concentration range of 1 to 270 ppm. We validated our method by analyzing a natural dry gas sample and comparing our results with those of two other independent analytical techniques, namely a CH_4-MultiGAS and a "Giggenbach bottle". When comparing the results between the CH_4-MultiGAS and the Picarro G2201-i, we measured differences of ~ 4 %, while when comparing the results between the Giggenbach bottle and the Picarro G2201-i, we measured differences of ~ 9 %. The results of these three techniques show excellent agreement within error of each other. Our study demonstrates that the Picarro G2201-i instrument can accurately and precisely measure CO_2, CH_4, and H_2S concentrations in the gas phase.

1. Introduction

The Picarro G2201-i gas analyzer is designed to measure $^{12}CO_2$, $^{13}CO_2$, $^{12}CH_4$, $^{14}CH_4$, and H_2O concentrations and isotopic compositions of $\delta^{13}C$-CO_2 and $\delta^{13}C$-CH_4. This instrument uses an analytical method known as Cavity Ring Down Spectroscopy (CRDS) which has been continuously improved since development in the 1980's (O'Keefe and Deacon, 1988). This method offers a fast and reliable approach to quantifying molecules at atmospheric concentrations. The CRDS technique allows for low drift and high precision (Crosson, 2008). This high precision is possible due to a rigorous selection of a specific spectroscopic line per molecule. Since each molecule is assigned a specific spectral line, multiple molecules can be analyzed

https://doi.org/10.5194/amt-2023-265
Preprint. Discussion started: 1 February 2024


Atmospheric Measurement Techniques Discussions

in one analysis simultaneously. The versatility of analyzing multiple species with the same instrument has made this technique popular in multiple disciplines in Earth Sciences such as soil science (e.g., Thurgood et al., 2014), ecology (e.g., Kulmatiski et al., 2010), hydrology (e.g., Jessen et al., 2014), ocean sciences (e.g., Klein and Welker, 2016), and atmospheric sciences (e.g., Tremoy et al., 2012).

The successful application of CRDS in these disciplines has inspired researchers to incorporate CRDS in volcanology. More specifically, Lucic et al. (2015), Malowany et al. (2017), Stix et al. (2017), and Hanson et al. (2018) used CRDS to analyze the isotopic composition of carbon dioxide in volcanic settings, while Ajayi and Ayers (2021) and Wei et al. (2021) have recently used CRDS to investigate the carbon isotope composition of methane in volcanic environments. The main disadvantage of using CRDS instruments in volcanic settings is that the presence of hydrogen sulfide (H_2S) produces a distortion on the spectral lines of CO_2 (Malowany et al., 2015).

This interference was first detected by Malowany et al. (2015) using a Picarro CRDS model G1101-i. According to Malowany et al. (2015) and Rella et al. (2015), the spectroscopic lines used to quantify the gas species and their isotopic compositions do not vary between the different models produced by Picarro. Therefore, it is expected that the presence of H_2S will also produce interference in the newer Picarro G2201-i instrument. Recent studies in volcanic environments using the G2201-i (e.g., Ajayi and Ayers, 2021; Hanson et al., 2018; Wei et al., 2021) acknowledged that the presence of H_2S produces interference in the $\delta^{13}C\text{-}CO_2$ measurements based on the Malowany et al. (2015) results. However, this interference has not yet been quantified in this newer instrument. Furthermore, the possible cross-interference between H_2S and $\delta^{13}C\text{-}CH_4$ has not been characterized in a Picarro G2201-i, even though Rella et al. (2015) identified a cross-interference for $\delta^{13}C\text{-}CH_4$ in the presence of H_2S using a Picarro G2132-i. In this contribution, we quantify the effects of H_2S on $\delta^{13}C\text{-}CO_2$ and $\delta^{13}C\text{-}CH_4$ in a G2201-i instrument.

Since H_2S causes these interferences, we use this interference to quantify H_2S concentrations with a Picarro G2201-i. Hence, we use the H_2S raw values from the Picarro instrument data processing package to measure H_2S accurately and precisely. Assan et al. (2017) and Defratyka et al. (2020) used the interference of ethene on $\delta^{13}C\text{-}CH_4$ to quantify ethane using a G2201-i. We followed their approach in order to quantify H_2S in the gas phase with the Picarro G2201-i. The possibility of measuring CO_2, CH_4, and H_2S concentrations in the gas phase using one instrument would significantly improve current analytical routines.

To use CRDS instruments in volcanic settings, we need to ensure that this technique will give us accurate and precise results despite the extreme conditions of such environments. Therefore, the objectives of this study are to a) detect and quantify the H_2S interference upon $^{12}CO_2$, $^{13}CO_2$, and $\delta^{13}C\text{-}CO_2$, b) compare the H_2S interference on $\delta^{13}C\text{-}CO_2$ between the G2201-i and the G1101-i based on the results from Malowany et al. (2015), c) detect and quantify possible cross-interferences on $\delta^{13}C\text{-}CH_4$ in the presence of H_2S, and d) quantify H_2S concentrations with a Picarro G2201-i.

https://doi.org/10.5194/amt-2023-265
Preprint. Discussion started: 1 February 2024

Atmospheric Measurement Techniques Discussions

2. Methods

This study presents the results of laboratory-based experiments to characterize the response of a Picarro G2201-i instrument to the presence of low and high H_2S concentrations. According to the manufacturer, other gases cause significant interference in this instrument. For example, C_2H_6 and NH_3 cause interference on $\delta^{13}C$-CH_4 as described in detail in the literature (Assan et al., 2017; Dalby et al., 2020; Defratyka et al., 2020; Rella et al., 2015). However, these gases are not considered in this study, as they are generally not present at significant levels in volcanic environments.

Our laboratory analysis consisted of mixing gas standards in Tedlar® bags to create a series of gas mixtures that allowed us to characterize the cross-interferences between two gases. The instrument response was evaluated for its full operational range with different gas combinations. We are interested in hydrothermal/volcanic compositions; therefore, we occasionally exceeded the limits of the operational range recommended by the manufacturer to explore the capability of the instrument in the context of gas compositions typically found in these settings (CO_2 > H_2S > CH_4).

2.1. Laboratory conditions

The laboratory experiments were run at a temperature of 20.5 ± 1.2 °C and an atmospheric pressure of 1010.6 ± 4.1 hPa at an altitude of 54 m.a.s.l. The gas flow of the instrument is about 25 cm^3 STP/min. The instrument's optical cavity is controlled at a temperature of 45 °C and a pressure of 148 Torr. The G2201-i instrument uses three spectral lines: 6029, 6057, and 6251 cm^{-1} (Defratyka et al., 2020). At a wavenumber of 6029 cm^{-1}, $^{13}CH_4$ and H_2O are measured, while the spectal line at 6057 cm^{-1} is used to measure $^{12}CH_4$ (Rella et al., 2015). The spectral line at 6251 cm^{-1} is used to measure $^{12}CO_2$ and $^{13}CO_2$ (Malowany et al., 2015). A syringe filter (Acrodisc® PTFE 1.0µm) was placed at the inlet to prevent particles from entering the system. A Tygon® tube was attached to the pump exhaust to vent the gases into the laboratory's fume hood, to prevent exposure to H_2S in the laboratory.

The G2201-i instrument operates in three different modes: 1) only CO_2, 2) only CH_4, and 3) CO_2 and CH_4 combined. All our experiments were conducted using the CO_2 and CH_4 simultaneous mode. Additionally, the CH_4 measurements have two operating modes: a) High Precision Mode (HP mode) and b) High Dynamic Range Mode (HR mode). The first is designed for low CH_4 concentrations from 1.8 to 12 ppm. The second mode is recommended for higher CH_4 concentrations in the range from 10 to 500 ppm. We followed these recommendations during our experiments, meaning that CH_4 concentrations lower than 10 ppm were analyzed using the High Precision Mode while higher CH_4 concentrations were analyzed using the High Dynamic Range. It is important to highlight that the CO_2 measurements have only one mode that covers a guaranteed range from 380 to 2000 ppm that is independent of the CH_4 mode in use.

https://doi.org/10.5194/amt-2023-265
Preprint. Discussion started: 1 February 2024

Atmospheric Measurement Techniques Discussions

2.2. Gas standards

The following gas standards were used: 995 ± 20 ppm CO_2 with an isotopic value of -28.66 ±0.43 ‰ relative to Vienna Pee Dee Belemnite (VPDB), 100 ± 1 % CO_2 with an isotopic value of -16.97 ± 0.19 ‰ relative to VPDB, 100 ± 1 % CH_4 with an isotopic value of -33.66 ± 1.9 ‰ relative to VPDB, and a 100 ± 2.5 ppm H_2S standard in N_2. Zero air was also used as the blank for the three gases (CO_2, CH_4, and H_2S) and was used to dilute the standards.

2.3. Gas mixtures

A 1 L Tedlar® bag was used to prepare gas mixtures of CO_2, CH_4, H_2S, and zero air. To achieve a quantitative dilution, the addition of each standard gas to the gas mixture was carefully measured. Syringes of 1 mL, 3 mL, 5 mL, 10 mL, 20 mL, 60 mL, and 120 mL were used to add aliquots of the standards for dilution, and a syringe of 1 L was used to add larger aliquots and to add the amount of zero air necessary to dilute the standard. To ensure proper mixing of the gas mixture, zero air was injected in two parts. First, half the zero air was injected into the bag. Then, an aliquot of the standard gas was added into the bag. Finally, the other half of the zero air was injected into the bag. This dilution process has associated uncertainties from ± 2% to ± 20% which are proportional to the dilution factor (aliquot of zero air/aliquot of gas standard). Higher dilution factors are associated with higher uncertainties; dilution factors > 2000 have uncertainties of ± 20 %, while dilution factors < 200 have uncertainties of ± 2 %.

Gas mixtures were prepared in the laboratory's fume hood immediately prior to analysis. The time between sample preparation and analysis never exceeded 5 minutes. To clean each Tedlar® bag between samples, the bag was filled with zero air gas and then emptied three times to avoid cross-contamination.

2.4. Analysis of samples

To monitor instrumental drift and define a baseline for the instrument, two control points (zero air and 995 ppm CO_2) were measured every day before starting a set of analyses. Zero air was used to define the blank level of the gases (i.e., 0 ppm CH_4, 0 ppm H_2S, and 4 ± 1 ppm CO_2). The results from the 995 ppm CO_2 standard analysis were used as the baseline for subsequent analysis.

The Picarro instrument performed continuous measurements while in operation, so between samples, the inlet was always exposed to room conditions to allow the signal to return to the background conditions in the laboratory.

Using the statistical tools of the Picarro instrument's interface, the $^{12}CO_2$ (ppm), $^{12}CH_4$ (ppm), $\delta^{13}C$-CO_2 (‰), and $\delta^{13}C$-CH_4 (‰) of each gas bag were averaged for the duration of the sample analysis (typically 10 minutes). This yielded a time-averaged measurement and a standard deviation for each sample.

https://doi.org/10.5194/amt-2023-265
Preprint. Discussion started: 1 February 2024


Atmospheric Measurement Techniques Discussions

2.5. Cross-interference experiments

After the control points were defined on a daily basis, we designed a set of experiments to identify cross-interference between two gases. For example, to quantify the interference between CO_2 and H_2S, we created a gas mixture of CO_2 and zero air. This gas mixture was analyzed by the Picarro G2201-i to define the CO_2 concentration and $\delta^{13}C$-CO_2 as a control. Then, increasing amounts of H_2S were added to this gas mixture to quantify the effects of H_2S on measurements of CO_2 concentrations and its isotopic composition. The same procedure was followed when the effect of H_2S on CH_4 was evaluated.

The gas mixtures spiked with H_2S were analyzed twice. First, the gas mixture was analyzed by scrubbing the H_2S before entering the system. To do this, a 10 cm copper tube containing copper filings was attached to the instrument's inlet, as was used by Malowany et al. (2015) to solve the interference detected in the measurements. Second, the gas mixture was analyzed without the copper tube. Between analyses, the inlet was exposed to room conditions to allow the signal to return to background levels. The differences in the measurements with and without the copper tube were used to estimate the effects of H_2S on CO_2 and CH_4 concentrations and their isotopic compositions.

2.6. Quantifying H_2S concentrations

We also explored the possibility of quantifying H_2S by using the "PPF_H2S" column from the Picarro instrument data processing package, which can be found in the output file that the analyzer automatically generates. During post-data analysis, the values from the "PPF_H2S" column were used to calculate an average and standard deviation for each analysis. This was done to simulate the statistical tools of the Picarro instrument's user interface. Following the method used by Assan et al. (2017) and Defratyka et al. (2020), we corrected and calibrated the "PPF_H2S" column to measure H_2S concentrations.

2.7. Measuring gas ratios of a natural hydrothermal sample

Once we defined the method to calibrate the H_2S raw value, we verified this technique by analyzing a natural hydrothermal gas sample. We collected a dry gas sample from an ambient temperature spring (~22.2 °C) with strong gas bubbling named Pailas Frías in Rincón de la Vieja volcano National Park, Costa Rica (sampling location coordinates: 10.7717°N, −85.3074°W). The concentrated gas was captured in pre-evacuated septum vials of 10 mL. The CO_2, CH_4, and H_2S gas composition has been described as ~80% CO_2, 0.01% CH_4, and ~ 1% H_2S (Salas-Navarro et al., 2022).

An aliquot of the sample was taken from the vial and diluted with zero air in a 1 L Tedlar® bag. This bag was then connected to the instrument inlet for approximately 5 minutes to measure the H_2S from the gas mixture. Then the bag was closed, and the instrument inlet was exposed to room conditions. Once all parameters had returned to room conditions, the same bag was connected to the instrument, but this time the gas mixture passed through the H_2S scrubber before reaching the inlet. In this way, we were able to measure the CO_2 and CH_4 concentrations without H_2S interference. Once the H_2S, CO_2, and CH_4 concentrations were accurately measured, the gas mixture was diluted by adding more zero air to the bag. Then the

https://doi.org/10.5194/amt-2023-265
Preprint. Discussion started: 1 February 2024


Atmospheric Measurement Techniques Discussions

procedure described above was repeated. The sample was progressively diluted until CH_4 concentrations were too low to be accurately measured. During post-data analysis, the PPF_H2S column was corrected and calibrated to obtain accurate H_2S concentrations.

The measured H_2S, CO_2, and CH_4 concentrations were used to calculate CO_2/H_2S, H_2S/CH_4, and CO_2/CH_4 ratios of the sample. These ratios can be calculated as the slope of a best-fit regression line (Aiuppa, 2005). The ratios calculated in this study were compared with the results of two other methods, a CH_4 Multi-component Gas Analysis System (CH_4-MultiGAS) (Salas-Navarro et al., 2022) and an evacuated glass bottle with caustic solution, also known as a "Giggenbach bottle" (Giggenbach, 1975). The CH_4 in the headspace of the Giggenbach bottle was analyzed by an Agilent 7890a gas chromatograph. The solution was oxidized and titrated with 0.1 N HCl to calculate CO_2, and H_2S was measured as SO_4 on a Dionex ICS-3000 ion chromatograph. The results of the CH_4-MultiGAS and the Giggenbach bottle analyses were reported by Salas-Navarro et al. (2022). The comparison among techniques was used to evaluate the accuracy and precision of our proposed quantification method for H_2S.

3. Results

3.1. Cross-interferences

The experiments show that presence of H_2S produces a linear effect on the $^{13}\delta C\text{-}CO_2$ raw value using the Picarro G2201-i (Fig. 1). The $\delta^{13}C\text{-}CO_2$ value decreased proportionally as the H_2S concentrations increased. For example, when adding 20000 ppb H_2S to the 995 ppm CO_2 gas standard with an accepted isotopic value of -28.66 ± 0.43‰, we measured a $\delta^{13}C\text{-}CO_2$ raw value of -985.2 ± 2.3 ‰, i.e., a difference of ~953 ‰ from the accepted isotopic value. The linear effect of increasing H_2S concentrations from 0 to 20000 ppb on $\delta^{13}C\text{-}CO_2$ ‰ is shown in Fig. 1A and is described with a slope of -0.0478 ± 0.0003. Figure 1A also shows the linear effect found by Malowany et al. (2015) using a Picarro G1101-i instrument described with a slope of -0.0268. The difference between these slopes is discussed in the next section.

Figure 1B shows the effect on $\delta^{13}C\text{-}CO_2$ ‰ at lower H_2S concentrations from 0 to 500 ppb. At these low H_2S concentrations, Fig. 1B shows a linear effect with a slope of -0.0414 ± 0.0014 which is 13% smaller compared to that from Fig. 1A. The similarity in the slopes in Fig. 1A and Fig. 1B shows that the effect of H_2S on $\delta^{13}C\text{-}CO_2$ is both linear and similar at low and high H_2S concentrations despite the higher uncertainties associated with the preparation of low H_2S concentrations.

As mentioned above, Malowany et al. (2015) showed that the interference caused by H_2S can be removed when adding a copper tube as an H_2S trap at the inlet of the Picarro G1101-i instrument. This solution is also effective for the Picarro G2201-i, as shown by the green triangles in Fig. 1B. The triangles represent the isotopic measurements after removing the H_2S using the copper tube.

The effect of H_2S on $\delta^{13}C\text{-}CO_2$ is produced because the measurement of $^{12}CO_2$ and $^{13}CO_2$ concentrations are affected differently by the presence of H_2S. When increasing H_2S, measured $^{12}CO_2$ concentration increases while $^{13}CO_2$ concentration

https://doi.org/10.5194/amt-2023-265
Preprint. Discussion started: 1 February 2024

Atmospheric Measurement Techniques Discussions

decreases. Figure S1 (Supplemental Materials) details these effects. Since the CO_2 concentrations are affected by the presence of H_2S, the linear interference of H_2S on $\delta^{13}C$-CO_2 is thus dependent on the CO_2 concentrations. Figure 2 shows that the H_2S interference is strongly dependent on the CO_2 concentration of the sample and enhanced at low CO_2 concentrations. Considering the linearity of this effect, the slopes in Fig. 1A (-0.0478 ± 0.0003) and Fig. 1B (-0.0414 ± 0.0014) were used to quantify the linear H_2S interference on $\delta^{13}C$-CO_2, where 30 ppb H_2S in 1000 ppm CO_2 causes an interference of ~1.0 ± 0.2 ‰ on the $\delta^{13}C$-CO_2 measurement.

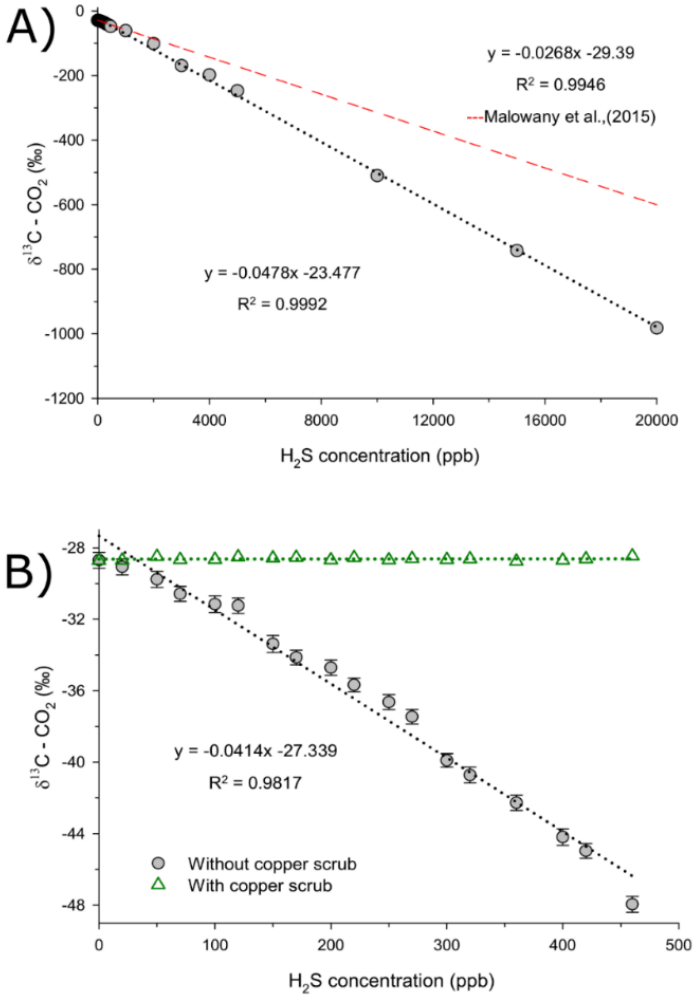

Figure 1. Effect of increasing the H_2S concentration a) from 0 to 20000 ppb H_2S and b) from 0 to 500 ppb H_2S on $\delta^{13}C$-CO_2 of the 995 ppm CO_2 standard with an accepted isotopic value of -28.66 ± 0.43‰. The gray circles represent the negative effect upon the $\delta^{13}C$-CO_2 value produced when increasing the H_2S concentrations in this study using a Picarro G2201-i instrument. The red line in A shows the slope from Malowany et al. (2015) using a Picarro G1101-i instrument. The green triangles in B represent the isotopic measurements after removing the H_2S using a copper tube as proposed by Malowany et al. (2015).

https://doi.org/10.5194/amt-2023-265
Preprint. Discussion started: 1 February 2024

Atmospheric Measurement Techniques Discussions

We further investigated if the presence of H_2S produces a similar effect on $\delta^{13}C$-CH_4. Figure 3 shows the results of adding H_2S to ~150 ppm CH_4 gas mixtures in the high dynamic range mode and adding H_2S to a ~7 ppm CH_4 gas mixture in the high precision mode. According to the manufacturer, the $\delta^{13}C$-CH_4 measurement has an error of <1.15 ‰ for the High Precision mode (HP mode) and a precision of <0.55 ‰ for the High Dynamic Range mode (HR mode)., which are shown in the error bars in Fig. 3. At ~150 ppm CH_4 it is not possible to identify a trend of increasing or decreasing $\delta^{13}C$-CH_4 when adding H_2S because all the values are within error of each other. On the other hand, at ~7 ppm CH_4, it is possible to observe a slight trend of decreasing $\delta^{13}C$-CH_4 when adding H_2S. When H_2S was increased from 0 to 20000 ppb, we measured a decrease in the $\delta^{13}C$-CH_4 value of ~1.66 ‰. Considering the reported error from the manufacturer (<1.15 ‰), we can argue that only ~0.5 ‰ is contributed by an interference on the spectral line of $\delta^{13}C$-CH_4 by H_2S. If we compare the $\delta^{13}C$-CH_4 value at 20000 ppb H_2S (-34.2 ± 1.2 ‰) with the accepted isotopic value of the CH_4 standard (-33.7 ± 1.9 ‰) we also find a difference of ~0.56 ‰. However, from our experiment it is not possible to measure a difference that is analytically distinguishable from the accepted isotopic value and the instrument's precision. Higher H_2S concentrations would be required to measure a significant difference. From Fig. 3 we conclude that $\delta^{13}C$-CH_4 is slightly affected by H_2S, and this effect is more prominent at low CH_4 concentrations and high H_2S concentrations.

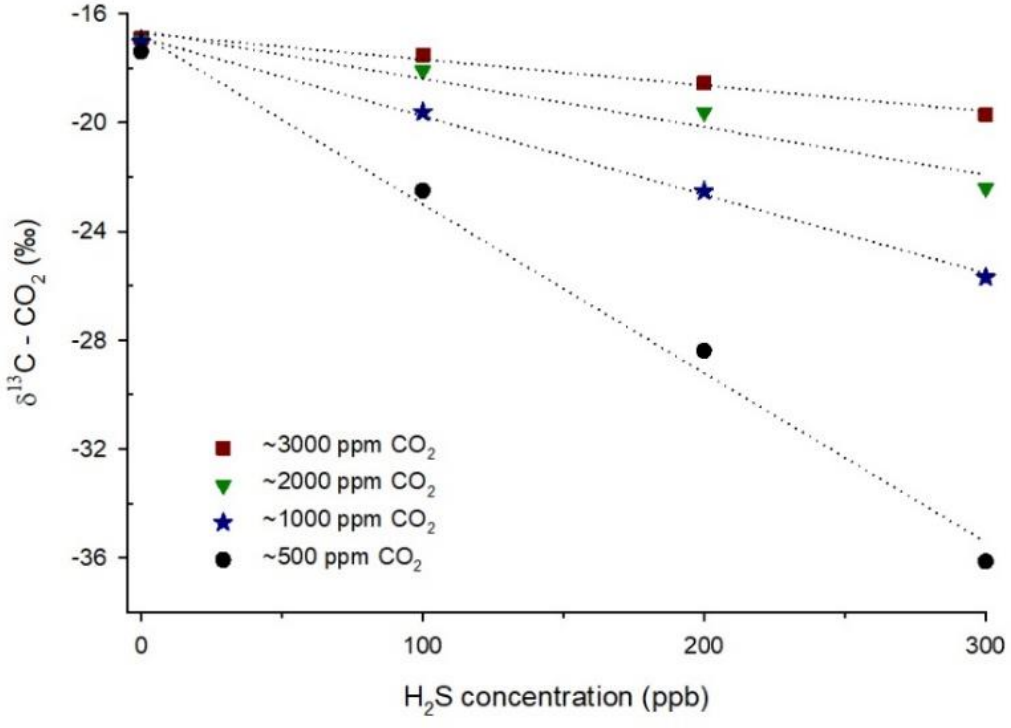

Figure 2. Effects of increasing the H_2S concentrations on the $\delta^{13}C$-CO_2 at varying CO_2 concentrations of a CO_2 standard gas with an accepted isotopic value of -16.97 ± 0.19 ‰.

https://doi.org/10.5194/amt-2023-265
Preprint. Discussion started: 1 February 2024

Atmospheric Measurement Techniques Discussions

Overall, it is important to highlight that the effect produced by H_2S on $\delta^{13}C\text{-}CO_2$ is much more significant than that produced on $\delta^{13}C\text{-}CH_4$, as shown in Fig. 1 and Fig. 3. In our experiments, very low concentrations of H_2S produced an effect on $\delta^{13}C\text{-}CO_2$, while >20 ppm H_2S would be required to produce a larger effect than the instruments' error on $\delta^{13}C\text{-}CH_4$ at 7 ppm CH_4.

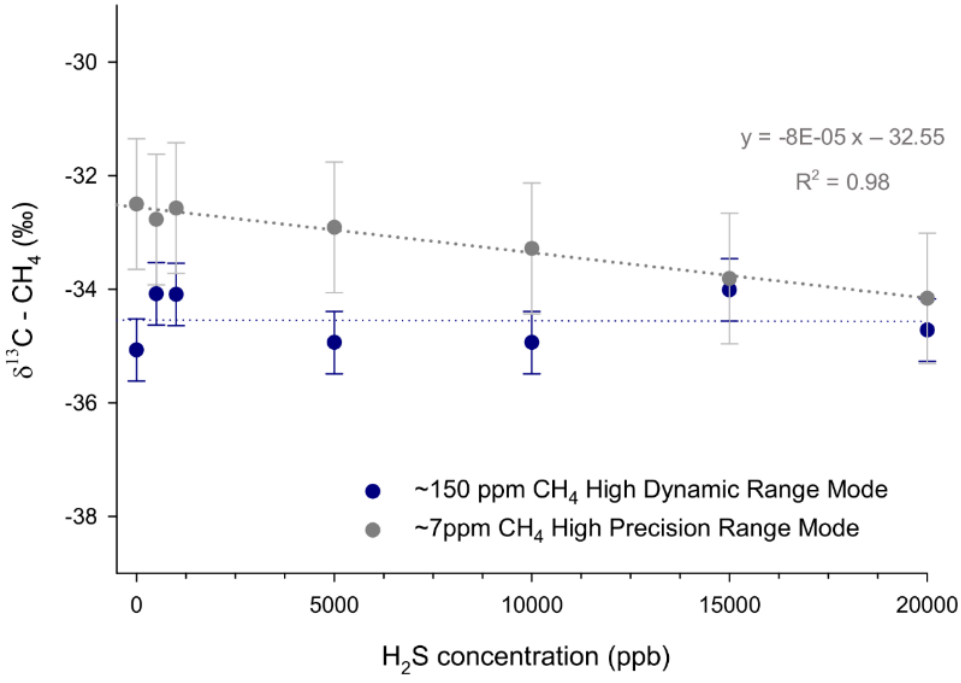

Figure 3. Isotopic measurements of $\delta^{13}C\text{-}CH_4$ ‰ of a CH_4 standard with an accepted value of -33.7 ± 1.9 ‰ when increasing the H_2S concentration from 0 to 20000 ppb. The error bars represent the instrument's precision reported by the manufacturer (< 1.15 ‰ for the High Precision Range Mode and < 0.55 ‰ for the High Dynamic Range Mode).

3.2. Quantifying H_2S concentrations

The values in the "PPF_H2S" column are registered in the G2201-i data processing package. Figure S2 shows a time series of laboratory experiments showing the changes in concentration of CH_4, CO_2 and the value of PPF_H2S of a mixture of gas standards and of our natural sample. "PPF_H2S" depends on the CH_4 and CO_2 concentrations. There is a positive correlation between the CO_2 concentration and the H_2S raw values. This means that the presence of CO_2 produces an increase in the reported H_2S raw concentration values even when H_2S is not present. By contrast, there is a negative correlation between the CH_4 concentration and the H_2S raw values, which means negative values of H_2S are measured when CH_4 is present.

https://doi.org/10.5194/amt-2023-265
Preprint. Discussion started: 1 February 2024

Atmospheric Measurement Techniques Discussions

In order to correct the H_2S raw value, the CH_4 interference on the "PPF_H2S" value was measured by creating a dilution series of CH_4 concentrations from 0 ppm to 200 ppm with no H_2S nor CO_2. An increase in the CH_4 concentrations results in lower H_2S raw values as shown in Fig. 4A. Above 20 ppm CH_4, the H_2S raw value became negative. This interference was characterized by a slope of -0.092 ± 0.002 with an R^2 value of 0.9982, as shown in Fig. 4A. The error bars represent the standard deviation of the H_2S raw value for the period when the bag was connected to the inlet. The error bars in Fig. 4A increase with CH_4 concentrations; at 0 ppm CH_4, the standard deviation of the H_2S raw value was ~1.8 ppm, while at 200 ppm CH_4, the standard deviation of the H_2S raw value was ~4 ppm.

The CO_2 interference on H_2S was measured by creating a second dilution series from 0 to 4000 ppm CO_2 with neither H_2S nor CH_4. An increase in the CO_2 concentrations results in higher reported values of H_2S. This interference was also found to be linear with a slope of 0.0028 ± 0.0001 and an R^2 value of 0.9935, as shown in Fig. 4B. The error bars represent the standard deviation for each measurement. In this case, an average standard deviation of ~1.7 ppm for the H_2S value was constant throughout the CO_2 concentration range.

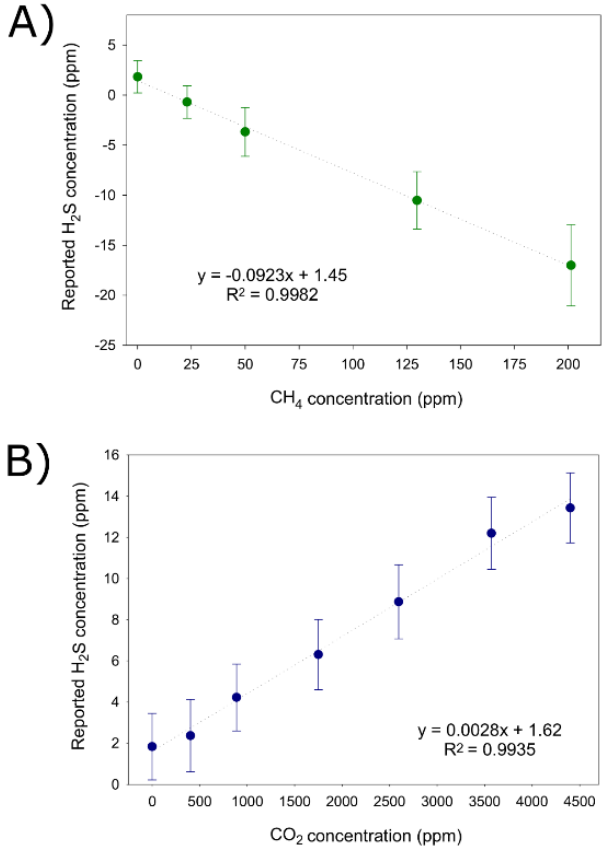

Figure 4. Linear regression between the reported H_2S ppm and a) 0 – 200 ppm CH_4 with no H_2S nor CO_2, and b) 0 – 4500 ppm CO_2 with no H_2S nor CH_4. The error bars in each plot denote the standard deviation of each measurement.

https://doi.org/10.5194/amt-2023-265
Preprint. Discussion started: 1 February 2024

Atmospheric Measurement Techniques Discussions

It is important to highlight that we kept our experiments at 0% water vapor. Therefore, the cross-interferences that could be caused by water vapor to the H_2S raw values are not considered in this calibration.

We can correct for these CO_2 and CH_4 interferences on the H_2S raw values by the following formula:

$$H_2S_{corrected} = H_2S_{raw\ value} - A * CO_2\ ppm - B * CH_4\ ppm \quad (1)$$

Where $A = 0.0028 \pm 0.0001$ and $B = -0.0923 \pm 0.0022$, which are the slopes of the linear regressions in Fig. 4. Once the H_2S raw value was corrected, the corrected value was calibrated by comparing the corrected value with the expected H_2S value of standard gas mixtures. The linear regressions for low and high concentrations are shown in Fig. 5A and Fig. 5B, respectively.

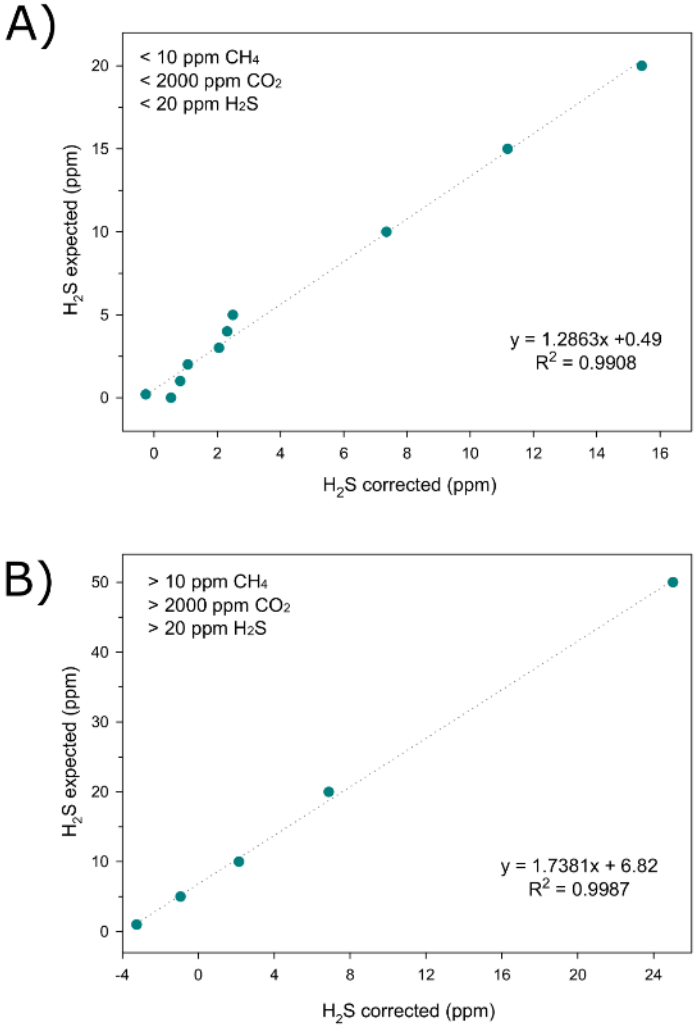

Figure 5. Calibration of the corrected H_2S value against the expected H_2S ppm a) for 0 to 10 ppm CH_4, 0 – 2000 ppm CO_2, and 1-20 ppm H_2S concentrations and b) for > 10 ppm CH_4, >2000 ppm CO_2, and > 20 ppm H_2S concentrations.

https://doi.org/10.5194/amt-2023-265
Preprint. Discussion started: 1 February 2024

Atmospheric Measurement Techniques Discussions

To calibrate H_2S in a range from 0 to 20 ppm H_2S, at CH_4 concentrations from 0 to 10 ppm and CO_2 concentrations from 0 to 2000 ppm, the following calibration equation is recommended:

$$H_2S_{calibrated} = 1.29 * H_2S_{corrected} + 0.49 \quad (2)$$

To calibrate H_2S at higher concentrations (> 2000 ppm CO_2, > 10 ppm CH_4, > 20 ppm H_2S) the following calibration equation is recommended:

$$H_2S_{calibrated} = 1.74 * H_2S_{corrected} + 6.8 \quad (3)$$

Using these equations, we were able to effectively calibrate the H_2S concentrations of gas standard mixtures. To confirm that this method is reliable for natural samples, we analyzed a direct sample of dry gas from the Pailas Frías hydrothermal cold spring. We calculated the CO_2/CH_4, CO_2/H_2S, and H_2S/CH_4 ratios of this natural sample (Table 1). Figure S3 shows the best-fit linear regressions used to calculate the gas ratio. The results shown in Table 1 are a comparison of the CO_2/CH_4, CO_2/H_2S, and H_2S/CH_4 ratios calculated with three different techniques, with excellent agreement within error of each other. The CO_2/H_2S and H_2S/CH_4 ratios calculated from the CH_4-MultiGAS are slightly higher than those from the Picarro G2201-i, with errors of 3.2 % and 4.4 %, respectively. The uncertainty in the calculated ratios from the Picarro G2201-i is higher than those from the CH_4-MultiGAS. The CO_2/CH_4 results from the evacuated bottle are lower than those of the CH_4-MultiGAS and the Picarro G2201-i. When comparing CO_2/H_2S, and H_2S/CH_4 ratios by the Picarro G2201-i and the evacuated bottle, we measured errors of -4.6 % and -13.0 %, respectively. This difference could be explained due to the complex combination of techniques required to determine the concentration of the molecules with the evacuated bottle technique (CH_4 by gas chromatography, CO_2 by titration, and H_2S by ion chromatography).

Table 1. Summary of CO_2/CH_4, CO_2/H_2S, and H_2S/CH_4 ratios from different sampling and analytical techniques. The results from the CH_4-MultiGAS and the evacuated bottles (Giggenbach bottles) are from Salas-Navarro et al. (2022).

	Picarro G2201-i	*CH_4-MultiGAS*	*Evacuated bottle*
CO_2/H_2S	90	93	86
±	16	3	-
R^2	0.94	0.98	-
H_2S/CH_4	87	91	77
±	33	9	-
R^2	0.78	0.92	-
CO_2/CH_4	8876	8333	6595
±	1621	809	-
R^2	0.94	0.92	-

https://doi.org/10.5194/amt-2023-265
Preprint. Discussion started: 1 February 2024


Atmospheric Measurement Techniques Discussions

4. Discussion

4.1. Cross-interferences: CO_2 vs H_2S

CO_2 concentrations and their isotopic compositions are significantly affected by H_2S. This interference is dependent upon both the CO_2 and H_2S concentrations as previously shown by Malowany et al. (2015). Measurements conducted at low CO_2 concentrations are more affected by the presence of H_2S, and higher H_2S concentrations produced larger deviations. These interferences are the result of an overlap of the specific spectral lines chosen by Picarro to avoid overlaps in typical atmospheric conditions (Malowany et al., 2015). However, at higher H_2S concentrations, such as those found in volcanic-hydrothermal environments, the spectral lines do overlap. Figure 6 displays the spectra of the gases considered in this study at wavenumbers of 6251 cm^{-1}, 6057 cm^{-1}, and 6029 cm^{-1} obtained from the HITRAN database (Gordon et al., 2022). Figure 6A shows the spectral line used for $^{12}CO_2$ and $^{13}CO_2$, illustrating the overlapping of the H_2S line with the $^{12}CO_2$ and $^{13}CO_2$ lines.

We found some differences when comparing our results of the Picarro G2201-i to those from Malowany et al. (2015) obtained using a Picarro G1101-i. For example, when we added 20 ppm H_2S to a 995 ppm CO_2 standard, we measured a $\delta^{13}C$-CO_2 value of -985.2 ± 2.3 ‰. However, for the same gas mixture, Malowany et al. (2015) measured an isotopic value of approximately -600 ‰. More specifically, when increasing H_2S concentrations from 0 to 20000 ppb, we obtained a slope of -0.0478 ± 0.0003 (see Fig. 1A). For the same range, Malowany et al. (2015) obtained a slope of -0.0268. When increasing the H_2S concentrations from 0 to 500 ppb, we obtained a slope of -0.0414 (see Fig. 1B), which is identical to that obtained by Malowany et al. (2015) for the same range. Our results indicate that the interference of H_2S on the $\delta^{13}C$-CO_2 is linear and similar at low and high H_2S concentrations.

Malowany et al. (2015) suggested that the difference in their slopes was due to the dilution of the CO_2 standard with large volumes of H_2S during sample preparation and mixing. In this study, our slopes differ by a small amount (13%). This may be due to improved sample preparation by using syringes to add a defined aliquot of H_2S standard instead of using the flux method of Malowany et al. (2015). Hence, we conclude that at low H_2S concentrations (0-500 ppb) the H_2S effect is the same in both instruments. We cannot directly compare the effect at higher H_2S concentrations (500 -20000 ppb), because of the errors incorporated in the dilution methodology in Malowany et al. (2015). The Picarro G1101-i does not measure $\delta^{13}C$-CH_4, therefore we cannot compare the two instruments in terms of carbon isotope compositions of methane isotopes.

4.2. Cross-interferences: CH_4 vs H_2S

Takriti et al. (2021) showed that the precision of carbon isotope measurements of methane increases with concentration. In other words, higher CH_4 concentrations led to smaller variability in the $\delta^{13}C$-CH_4 measurements, while lower CH_4 concentrations result in higher variability and therefore higher standard deviations. According to the instrument specifications, $\delta^{13}C$-CH_4 ‰ has a precision of <1.15 ‰ for the High Precision mode (HP mode) and a precision of <0.55 ‰ for the High Dynamic Range mode (HR mode). The higher variability of reported $\delta^{13}C$-CH_4 values at low CH_4 concentrations thus makes

https://doi.org/10.5194/amt-2023-265
Preprint. Discussion started: 1 February 2024

Atmospheric Measurement Techniques Discussions

it challenging to detect interferences at these levels. According to Rella et al. (2015), there is a distortion in the δ^{13}C-CH_4 absorption spectrum caused by H_2S.These authors defined an effect of <0.2 ‰ on δ^{13}C-CH_4 per 1 ppm H_2S in 1 ppm CH_4 using a Picarro model G2132-i, which was configured to measure δ^{13}C-CH_4 and CH_4, CO_2, and H_2O concentrations. They defined this effect as proportional to the H_2S concentration and inversely proportional to the CH_4 concentration. For instance, the higher the methane concentration, the smaller the effect produced by a given concentration of H_2S.

Our findings agree with those of Takriti et al. (2021) and Rella et al. (2015). As shown in Fig. 3, at high methane concentrations measured δ^{13}C-CH_4 is less variable, and we do not observe an effect on the δ^{13}C-CH_4 value with increasing H_2S concentrations. Using Rella et al. (2015)'s defined effect (<0.2 ‰ on δ^{13}C-CH_4 per 1 H_2S ppm in 1 CH_4 ppm), 20 ppm of H_2S in a gas mixture of ~150 ppm CH_4 should produce a shift in the δ^{13}C-CH_4 value of $[0.2\ ‰\ CH_4\ ppm * (H_2S\ ppm)^{-1}] \times [20\ ppm\ H_2S]/[150\ ppm CH_4] = -0.027‰$. By contrast, at lower CH_4 concentrations, measured δ^{13}C-CH_4 is more variable, and we also observe a slightly decreasing trend of δ^{13}C-CH_4 with increasing H_2S. In fact, when we added 20 ppm of H_2S to a 7 ppm CH_4 gas mixture, we measured a difference of 0.56 ‰ from the accepted isotopic value (-33.7 ± 1.9 ‰) of the CH_4 gas standard. This difference agrees with Rella et al. (2015)'s defined effect, where 20 ppm of H_2S in a gas mixture of ~7 ppm CH_4 should produce a shift in the δ^{13}C-CH_4 value by $[0.2\ ‰\ CH_4\ ppm * (H_2S\ ppm)^{-1}] \times [20\ ppm\ H_2S]/[7\ ppm CH_4] = -0.57‰$. However, as mentioned above, these differences are within the instrument's precision.

In order to verify these findings, we considered the spectral lines for methane. Figure 6B and 6C show the spectra for $^{12}CH_4$ and $^{13}CH_4$ at 6057 cm^{-1} and 6029 cm^{-1} respectively. At 6029 cm^{-1} the spectral line of $^{13}CH_4$ is slightly overlapped by H_2S, while the spectral line of $^{12}CH_4$ is not overlapped at 6057 cm^{-1}. This overlap at 6029 cm^{-1} explains the slight decrease in δ^{13}C-CH_4 shown in Fig. 3 and the 0.56 ‰ difference estimated above.

Based on these results, we conclude that the addition of H_2S produces a small interference on the δ^{13}C-CH_4 values. As proposed by Rella et al. (2015), we suggest that the H_2S interference on the δ^{13}C-CH_4 values using a G2201-i can be defined as < 0.2 ‰ on δ^{13}C-CH_4 per 1 ppm H_2S in 1 ppm CH_4. However, from the experiments that we conducted in this study, it is not possible to clearly distinguish this interference outside of the instrument's error. The differences measured in this study are within the precision reported by the manufacturer for the high precision mode and for the high dynamic range mode.

Other experiments can be performed to verify this conclusion. For example, at 7 ppm CH_4 concentration, more than 20 ppm H_2S will be necessary to generate a significant effect on δ^{13}C-CH_4. However, we were not able to perform experiments at H_2S concentrations higher than 20 ppm because the H_2S gas standard includes small traces of CH_4 that could lead to erroneous conclusions. Another experiment could be performed at 2 ppm CH_4 concentration (atmospheric conditions), where 20 ppm H_2S could cause an effect of ~2 ‰, which would be higher than the precision reported by the manufacturer. We did not conduct experiments at CH_4 concentrations lower than ~7 ppm, because preparing such dilutions of our 100 % CH_4 gas standard would likely be unreliable. Further experiments could be conducted with significantly higher CH_4 concentrations (i.e., CH_4>CO_2).

https://doi.org/10.5194/amt-2023-265
Preprint. Discussion started: 1 February 2024

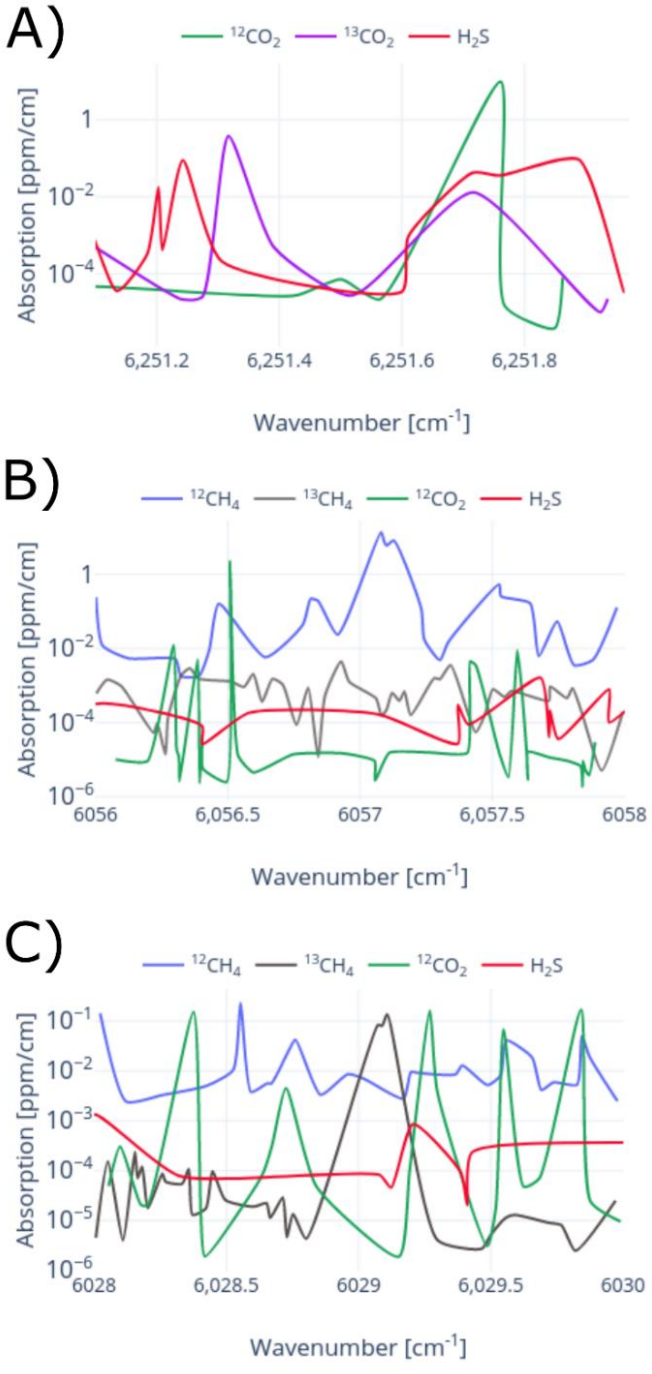

Figure 6. Spectral data for 400 ppm CO_2, 2 ppm CH_4, and 1 ppm H_2S at a pressure of 148 Torr and a temperature of 45 °C. A) Spectra of $^{12}CO_2$, $^{13}CO_2$, and H_2S at a wavenumber of 6251 cm^{-1}, b) Spectra of $^{12}CH_4$, $^{13}CH_4$, $^{12}CO_2$, and H_2S at 6057 cm^{-1}, and c) Spectra of $^{12}CH_4$, $^{13}CH_4$, $^{12}CO_2$, and H_2S at 6029 cm^{-1}. The spectra were obtained from the HITRAN spectra database (Gordon et al., 2022).

https://doi.org/10.5194/amt-2023-265
Preprint. Discussion started: 1 February 2024


Atmospheric Measurement Techniques Discussions

4.3. Quantifying H_2S concentrations

Our results show that it is possible to quantitatively measure H_2S with the Picarro G2201-i instrument. We focused our study on highly concentrated gas mixtures to represent volcanic environments. We also presented the results of a particularly challenging natural sample from a cold hydrothermal spring. This sample is challenging due to the high proportion of CO_2 relative to CH_4. Therefore, a large dilution was necessary to measure CO_2 within the instrument's operational range. As mentioned before, a large dilution is associated with higher uncertainties in the gas mixture preparation. Additionally, this natural gas sample contained large amounts of H_2S, and multiple H_2S traps were required to fully scrub all the H_2S before gas entered the instrument to accurately measure the CO_2 and CH_4 concentrations. Since we were able to successfully characterize this analytically difficult sample, we believe that other samples with lower CO_2/H_2S and CO_2/CH_4 ratios can be characterized more easily, with smaller errors compared to other techniques.

We were able to quantify H_2S in a concentration range from 1 to ~270 ppm. It is important to highlight that our H_2S gas standard was used to calibrate H_2S from 1 to 100 ppm, while the natural gas sample was used to calibrate H_2S from 100 to 270 ppm. As we mentioned above, our H_2S standard includes detectable CH_4 at H_2S > 20 ppm. Using Eq. (1) we corrected the effect of CH_4 on the H_2S raw value at H_2S concentrations from 20 to 100 ppm.

From 100 to 270 ppm, H_2S was defined using the natural sample. As shown in Fig. S2, at these higher concentrations, we exceeded the recommended operational range of the instrument because of the complexity of our natural sample. Despite this, the calculated CO_2/H_2S ratio shows a good correlation with $R^2 = 0.94$. We did not attempt to calculate higher concentrations of H_2S because this would have required injecting exceedingly high concentrations of CO_2 into the system due to the composition of our natural sample. Therefore, we avoided compromising the functionality of the instrument. H_2S concentrations higher than 270 ppm could be assessed by using more concentrated standards, or alternatively by using a natural sample with a CO_2/H_2S ratio lower than the one used in this study.

The raw H_2S signal is noisy (see error bars in Fig. 4 and Fig. S2A), thus the detection and quantification of low H_2S concentrations are challenging. The standard deviation of the "blank" (i.e., zero air) is ~1.6 ppm. This standard deviation does not change when CO_2 is present. However, the presence of CH_4 can double it. Thus, we used a moving average to improve the signal-to-noise ratio at low H_2S concentrations. We applied a 20-second running average to the H_2S raw values, decreasing the noise and allowing us to measure H_2S concentrations as low as 1 ppm. We recognize that the uncertainty of this measurement is high for low H_2S concentrations.

Below 1 ppm, H_2S concentrations can be estimated using the calculated interference of ~1.0 ± 0.2 ‰ $\delta^{13}C\text{-}CO_2$ ‰ per 30 ppb H_2S in 1000 ppm CO_2 presented above. By running the sample with and without the H_2S trap, we can define the CO_2 concentrations and the difference in $\delta^{13}C\text{-}CO_2$ ‰. Using this information, we can estimate the H_2S concentration at ppb levels. We recommend this method for H_2S concentrations from 0 to 1 ppm. This estimation does not consider the CH_4 concentration; therefore, the H_2S concentration obtained using this method is an approximation. For higher H_2S concentrations, we recommend the method using Eq. (1), (2), or (3).

https://doi.org/10.5194/amt-2023-265
Preprint. Discussion started: 1 February 2024

Atmospheric Measurement Techniques Discussions

In this study, we used a natural hydrothermal gas sample for which gas ratios (CO_2/CH_4, CO_2/H_2S, and H_2S/CH_4) were calculated with two different techniques by Salas-Navarro et al. (2022). When we compare these techniques with our method in Table 1, we observe good agreement among the calculated ratios from the different techniques. However, the uncertainty of the ratios measured by the Picarro G2201-i is higher than that of the CH_4-MultiGAS. These higher uncertainties could be related to the noisy H_2S raw signal and the low CH_4 concentrations. To reduce the signal-to-noise ratio, moving averages can be applied to the H_2S raw signal. We did not use a moving average for the measurements of the natural sample to keep the proposed method as simple as possible. Higher CH_4 concentrations would also reduce the uncertainty of these ratios.

Figure 7 compares the three techniques in a ternary diagram. The data cluster closely together, showing good agreement among techniques. This comparison demonstrates that the Picarro G2201-i can be used to accurately define the composition of a natural hydrothermal gas sample in terms of its CO_2-CH_4-H_2S components. The agreement in these results indicates that this method has the potential to become a useful laboratory tool for analyzing volcanic and hydrothermal gases.

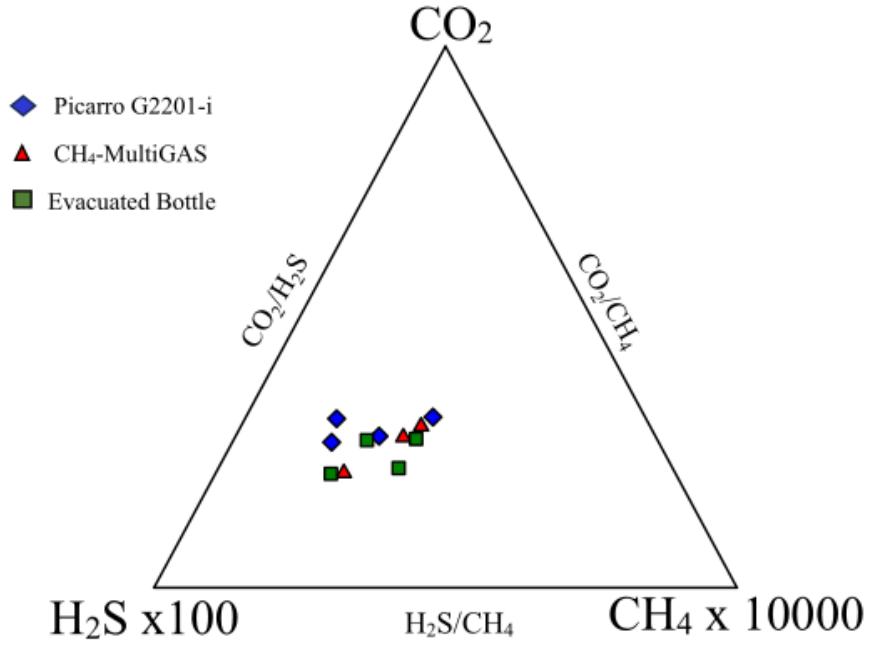

Figure 7. Ternary diagram showing the gas composition of the natural sample. The green squares show the results from the evacuated or "Giggenbach" bottle technique, the red triangles show the measurements with the CH_4-MultiGAS, and the blue diamonds show the results from the analysis with the Picarro G2201-i. The CO_2/CH_4, CO_2/H_2S, and H_2S/CH_4 values are listed in Table 1.

https://doi.org/10.5194/amt-2023-265
Preprint. Discussion started: 1 February 2024


Atmospheric Measurement Techniques Discussions

5. Conclusions

Due to the distortion of the absorption spectral lines, cross-interferences among CO_2, CH_4, and H_2S were detected using the Picarro G2201-i. The presence of H_2S produces a significant interference for CO_2 concentrations and isotopic compositions. This effect is dependent on CO_2 concentrations; at lower CO_2 concentrations, the effect is larger. The presence of H_2S also produces a smaller interference on $\delta^{13}C$-CH_4 which is also dependent on CH_4 concentration. At low methane concentrations, H_2S will produce a larger effect on the measurement of the carbon isotope composition of methane.

These H_2S interferences allowed us to develop a novel approach to quantify H_2S concentrations using the G2201-i instrument. It is important to note that a possible cross-interference of water vapor or other gases on the H_2S signal might be present but was not assessed in the present study. This issue should be explored further. Experiments with higher CH_4 concentrations could expand the findings of our study. The experiments of this study were all performed in a laboratory setting. Further experiments could evaluate our method in the field.

Our approach demonstrates the potential of cavity ringdown spectrometers to simultaneously and rapidly measure CO_2, CH_4, and H_2S in volcanic and hydrothermal gas samples, which could be a powerful method for volcano monitoring. In minutes, it is possible to analyze a sample both with and without an H_2S trap. The sample is analyzed with a copper tube to measure the correct CO_2 and CH_4 concentrations, then the sample is analyzed again without the copper tube to measure the H_2S concentration. The raw H_2S concentration values are corrected using Eq. (1) and then calibrated with Eq. (2), or Eq. (3) depending on the concentration range. Using our proposed method, it is possible to determine the CO_2/CH_4, CO_2/H_2S, and H_2S/CH_4 ratios of a dry gas sample within 20 minutes using a single instrument.

Data availability

All raw data can be provided by the corresponding author upon request.

Author contributions

Jessica Salas-Navarro: Conceptualization, Data curation, Formal analysis, Methodology, Investigation, Validation, Visualization, Project administration, Writing – original draft.

John Stix: Conceptualization, Methodology, Investigation, Funding acquisition, Supervision, Resources, Writing – review & editing,

J. Maarten de Moor: Conceptualization, Methodology, Validation, Investigation, Funding acquisition, Supervision, Resources, Writing – review & editing,

Competing interests

The authors declare that they have no known competing financial interests or personal relationships that could have appeared to influence the work reported in this paper.

Acknowledgements

We thank Gregor Lucic and John Hoffnagle from Picarro Inc. for useful comments. We gratefully acknowledge the help of Alejandro Rodríguez in the collection of direct samples. We are grateful to Dr. Hans Osthoff (editor) for detailed comments, which allowed us to make substantive improvements to this manuscript.

Financial support

This work was supported by Discovery grants to JS from the Natural Sciences and Engineering Research Council of Canada (NSERC). MdM gratefully acknowledges support from NSF-FRES award 2121637, from the Costa Rican Ley Transitorio 8933 and from Universidad Nacional, Costa Rica.

References

Aiuppa, A.: Chemical mapping of a fumarolic field: La Fossa Crater, Vulcano Island (Aeolian Islands, Italy), Geophys. Res. Lett., 32, https://doi.org/10.1029/2005gl023207, 2005.

Ajayi, M. and Ayers, J. C.: CH_4 and CO_2 diffuse gas emissions before, during and after a Steamboat Geyser eruption, J. Volcanol. Geotherm. Res., 414, 107233, https://doi.org/10.1016/j.jvolgeores.2021.107233, 2021.

Assan, S., Baudic, A., Guemri, A., Ciais, P., Gros, V., and Vogel, F. R.: Characterization of interferences to in situ observations of $\delta^{13}CH_4$ and C_2H_6 when using a cavity ring-down spectrometer at industrial sites, Atmos. Meas. Tech., 10, 2077-2091, https://doi.org/10.5194/amt-10-2077-2017, 2017.

Crosson, E. R.: A cavity ring-down analyzer for measuring atmospheric levels of methane, carbon dioxide, and water vapor, Appl. Phys. B, 92, 403-408, https://doi.org/10.1007/s00340-008-3135-y, 2008.

Dalby, F. R., Fuchs, A., and Feilberg, A.: Methanogenic pathways and $\delta^{13}C$ values from swine manure with a cavity ring-down spectrometer: Ammonia cross-interference and carbon isotope labeling, Rapid Communications in Mass Spectrometry, 34, e8628, https://doi.org/10.1002/rcm.8628, 2020.

Defratyka, S. M., Paris, J. D., Yver-Kwok, C., Loeb, D., France, J., Helmore, J., Yarrow, N., Gros, V., and Bousquet, P.: Ethane measurement by Picarro CRDS G2201-i in laboratory and field conditions: potential and limitations, Atmos. Meas. Tech. Discuss., 2020, 1-24, https://doi.org/10.5194/amt-2020-410, 2020

Giggenbach, W. F.: A simple method for the collection and analysis of volcanic gas samples, Bull. Volcanol., 39, 132-145, https://doi.org/10.1007/BF02596953, 1975.

Gordon, I. E., Rothman, L. S., Hargreaves, R. J., Hashemi, R., Karlovets, E. V., Skinner, F. M., Conway, E. K., Hill, C., Kochanov, R. V., Tan, Y., Wcisło, P., Finenko, A. A., Nelson, K., Bernath, P. F., Birk, M., Boudon, V., Campargue, A., Chance, K. V., Coustenis, A., Drouin, B. J., Flaud, J. M., Gamache, R. R., Hodges, J. T., Jacquemart, D., Mlawer, E. J., Nikitin,

https://doi.org/10.5194/amt-2023-265
Preprint. Discussion started: 1 February 2024

A. V., Perevalov, V. I., Rotger, M., Tennyson, J., Toon, G. C., Tran, H., Tyuterev, V. G., Adkins, E. M., Baker, A., Barbe, A., Canè, E., Császár, A. G., Dudaryonok, A., Egorov, O., Fleisher, A. J., Fleurbaey, H., Foltynowicz, A., Furtenbacher, T., Harrison, J. J., Hartmann, J. M., Horneman, V. M., Huang, X., Karman, T., Karns, J., Kassi, S., Kleiner, I., Kofman, V., Kwabia–Tchana, F., Lavrentieva, N. N., Lee, T. J., Long, D. A., Lukashevskaya, A. A., Lyulin, O. M., Makhnev, V. Y., Matt, W., Massie, S. T., Melosso, M., Mikhailenko, S. N., Mondelain, D., Müller, H. S. P., Naumenko, O. V., Perrin, A., Polyansky, O. L., Raddaoui, E., Raston, P. L., Reed, Z. D., Rey, M., Richard, C., Tóbiás, R., Sadiek, I., Schwenke, D. W., Starikova, E., Sung, K., Tamassia, F., Tashkun, S. A., Vander Auwera, J., Vasilenko, I. A., Vigasin, A. A., Villanueva, G. L., Vispoel, B., Wagner, G., Yachmenev, A., and Yurchenko, S. N.: The HITRAN2020 molecular spectroscopic database, Journal of Quantitative Spectroscopy and Radiative Transfer, 277, 107949, https://doi.org/10.1016/j.jqsrt.2021.107949, 2022.

Hanson, M. C., Oze, C., Werner, C., and Horton, T. W.: Soil $\delta^{13}C$-CO_2 and CO_2 flux in the H_2S-rich Rotorua hydrothermal system utilizing Cavity Ring Down Spectroscopy, J. Volcanol. Geotherm. Res., 358, 252-260, https://doi.org/10.1016/j.jvolgeores.2018.05.018, 2018.

Jessen, S., Holmslykke, H. D., Rasmussen, K., Richardt, N., and Holm, P. E.: Hydrology and pore water chemistry in a permafrost wetland, Ilulissat, Greenland, Water Res. Res., 50, 4760-4774, https://doi.org/10.1002/2013WR014376, 2014.

Klein, E. S. and Welker, J. M.: Influence of sea ice on ocean water vapor isotopes and Greenland ice core records, Geophys. Res. Lett., 43, 12,475-412,483, https://doi.org/10.1002/2016GL071748, 2016.

Kulmatiski, A., Beard, K. H., Verweij, R. J. T., and February, E. C.: A depth-controlled tracer technique measures vertical, horizontal and temporal patterns of water use by trees and grasses in a subtropical savanna, New Phytologist, 188, 199-209, https://doi.org/10.1111/j.1469-8137.2010.03338.x, 2010.

Lucic, G., Stix, J., and Wing, B.: Structural controls on the emission of magmatic carbon dioxide gas, Long Valley Caldera, USA, J. of Geophys. Res: Solid Earth, 120, 2262-2278, https://doi.org/10.1002/2014JB011760, 2015.

Malowany, K., Stix, J., Van Pelt, A., and Lucic, G.: H_2S interference on CO_2 isotopic measurements using a Picarro G1101-i cavity ring-down spectrometer, Atmos. Meas. Tech., 8, 4075-4082, https://doi-org/10.5194/amt-8-4075-2015, 2015.

Malowany, K. S., Stix, J., de Moor, J. M., Chu, K., Lacrampe-Couloume, G., and Sherwood Lollar, B.: Carbon isotope systematics of Turrialba volcano, Costa Rica, using a portable cavity ring-down spectrometer, Geochem., Geophys., Geosyst., 18, 2769-2784, https://doi.org/10.1002/2017GC006856, 2017.

O'Keefe, A. and Deacon, D. A. G.: Cavity ring-down optical spectrometer for absorption measurements using pulsed laser sources, Rev. Sci. Instr., 59, 2544-2551, https://doi-org/10.1063/1.1139895, 1988.

Rella, C. W., Hoffnagle, J., He, Y., and Tajima, S.: Local- and regional-scale measurements of CH_4, $\delta^{13}CH_4$, and C_2H_6 in the Uintah Basin using a mobile stable isotope analyzer, Atmos. Meas. Tech., 8, 4539-4559, https://doi-org/10.5194/amt-8-4539-2015, 2015.

Salas-Navarro, J., Stix, J., and de Moor, J. M.: A new Multi-GAS system for continuous monitoring of CO_2/CH_4 ratios at active volcanoes, J. Volcanol. Geotherm. Res., 107533, https://doi.org/10.1016/j.jvolgeores.2022.107533, 2022.

Stix, J., Lucic, G., and Malowany, K.: Near real-time field measurements of $\delta^{13}C$ in CO_2 from volcanoes, Bull. Volcanol., 79, 62, https://doi-org/10.1007/s00445-017-1144-6, 2017.

Takriti, M., Wynn, P. M., Elias, D. M. O., Ward, S. E., Oakley, S., and McNamara, N. P.: Mobile methane measurements: Effects of instrument specifications on data interpretation, reproducibility, and isotopic precision, Atm. Env., 246, 118067, https://doi.org/10.1016/j.atmosenv.2020.118067, 2021.

https://doi.org/10.5194/amt-2023-265
Preprint. Discussion started: 1 February 2024

Atmospheric Measurement Techniques Discussions

Thurgood, A., Singh, B., Jones, E., and Barbour, M. M.: Temperature sensitivity of soil and root respiration in contrasting soils, Plant and Soil, 382, 253-267, https://doi-org/10.1007/s11104-014-2159-9, 2014.

Tremoy, G., Vimeux, F., Mayaki, S., Souley, I., Cattani, O., Risi, C., Favreau, G., and Oi, M.: A 1-year long $\delta^{18}O$ record of water vapor in Niamey (Niger) reveals insightful atmospheric processes at different timescales, Geophys. Res. Lett., 39, https://doi.org/10.1029/2012GL051298, 2012.

Wei, F., Xu, J., Kong, Q., Liu, S., Xu, D., and Pan, B.: Sources of CH_4 with variable carbon isotopes from Changbaishan volcano in NE China: Implications for the feeding system, J. Volcanol. Geotherm. Res., 419, 107355, https://doi.org/10.1016/j.jvolgeores.2021.107355, 2021.